Band structure engineering of a nonlinear optical response in semiconductor superlattices

1990 J. Phys.: Condens. Matter 2 4879

(http://iopscience.iop.org/0953-8984/2/22/009)

J. Phys.: Condens. Matter 2 (1990) 4879–4893. Printed in the UK

Band structure engineering of a non-linear optical response in semiconductor superlattices

I Morrison and M Jaros

Department of Physics, The University of Newcastle upon Tyne, Newcastle upon Tyne NE1 7RU, UK

Received 18 December 1989, in final form 23 February 1990

Abstract. We show that the non-linear response of certain direct gap semiconductor superlattices is greatly enhanced when the separation of the lowest conduction bands is comparable with the magnitude of the principal gap. The mechanism which results in this enhancement is virtual transitions to higher subbands. Examples of $(InAs)_{1-x}(GaSb)_x/AlSb$ superlattices expected to exhibit the enhanced non-linear response in the near-infrared region of the spectrum are presented. We also investigate non-linear response in semiconductor superlattices at ultrashort times ($\sim$ 100 fs). In our scheme a full account is given for the first time of band structure effects upon transients. We then use a three-level model to determine the conditions under which predictions, based on the steady-state response theory and the golden rule, break down in structures with closely spaced energy levels.

1. Introduction

We recently proposed a new mechanism which is expected to lead to greatly enhanced third-order optical susceptibilities in semiconductor superlattices (Morrison *et al* 1989). This new mechanism involves virtual excitations to higher subbands. Such processes have not been examined in the literature, although they can be readily understood in terms of the general theory of non-linear optical phenomena (Shen 1984, Flyzanis 1975, Wherret 1983, Kelly 1963). In particular they do not belong to the class of excitonic non-linearities which have recently dominated the literature on the subject (Haug and Schmitt-Rink 1985, Chemla 1988, Miller 1989, Wolf *et al* 1987, Chang 1985). In the previous report we proposed specific InAs–ZnTe and CdTe–$Hg_{1-x}Cd_xTe$ superlattice structures expected to exhibit an enhancement of the non-linear response due to this mechanism. The usefulness of the above structures is limited due to the difficulty encountered in growing samples with dislocation free interfaces. In this paper we, first of all, describe in greater detail the new mechanism expected to enhance the non-linear response. We also propose several $(InAs)_{1-x}(GaSb)_x/AlSb$ superlattices expected to display the large non-linear response. These structures do not have the growth problems associated with the previously proposed superlattices and have the added advantage that their optical gaps span the near-infrared region of the spectrum used in long distance optical communications.

Secondly, we present a study of the transient features expected in such structures upon application of very short laser pulses. To achieve this end we employ standard quantum mechanical techniques familiar to the materials scientist. We determine

0953-8984/90/224879+15$03.50

the regime of energy separations versus pulse length at which the Fermi golden rule breaks down and illustrate quantitatively the consequences of this breakdown upon the transient response. We recover the transient familiar from earlier studies of molecular and bulk systems and show that in the structures proposed above this breakdown is of no practical significance. This means that, in this case, the conventional models of higher-order susceptibilities (Shen 1984, Flyzanis 1975, Wherret 1983, Kelly 1963), which assume a steady-state response and related approximations, remain valid for pulses longer than 50 fs, (50×10^{-15} s). However, since the essence of the higher-order mechanism stems from the availability of strong dipole matrix elements between higher subbands, and since the momentum wavefunctions of such subbands are broadened by quantum effects at the interfaces, we conclude that a full band structure approach will be needed to provide a quantitative account of such non-linear response. This is in good accord with the conclusions obtained in calculations similar to ours on bulk semiconductors (Wherret 1983, Fong and Shen 1975). It is, however, in contrast with the band blocking mechanism of changing the refractive index in which the effects of higher subbands are not very important. In our assessment of the transient response we also consider band structure effects such as those that occur when superlattice states derived from different points of the bulk Brillouin zone interact (Brown *et al* 1987). No such transient effects have been considered in the literature.

2. Superlattices with a large virtual non-linearity

There are a number of processes that can bring about large optical non-linearities in man-made semiconductor structures. Nonlinear here means that the refractive index of the semiconductor microstructure depends on the intensity of the applied field. A large intensity dependence of the refractive index is desirable as it provides the basis of optical signal processing (Thylén 1988). The most exploited mechanism for generating optical non-linearities in semiconductor microstructures is band filling. The change in the refractive index is caused by blocking the quantum states normally available in the conduction band. In order to observe non-linearity due to such processes, a high incident field is needed to produce the required concentrations of electrons and holes. Hence the change in refractive index is achieved at the cost of strong energy dissipation (absorption) in the material. This large power requirement is a major disadvantage in device applications. Another source of non-linearity in semiconductors can be described by the virtual excitation of electrons to higher bands via many-photon processes, see figure 1 for example. Such virtual transitions can also be used to describe the excitonic energy shifts observed in the optical Stark effect (Frohlich *et al* 1987, Knox *et al* 1989, Peyghambarian 1989). These processes are not accompanied by the high absorption rates associated with the band filling effect. It is with the virtual mechanism that we shall be concerned in this study. In bulk semiconductors, this non-linearity is generally too small to be useful for applications. However, we shall show it is possible to design semiconductor superlattices such that the separations of energy levels and the transition probabilities between them satisfy the requirements for a significant enhancement of the non-linear response.

A large field dependence of the refractive index requires a large component of $\chi^{(3)}$ at $\omega = \omega - \omega + \omega$ (Haug 1988), where ω is the frequency of the incident radiation. This component of $\chi^{(3)}$ causes a response of the system at the exciting frequency which results in refraction. The expression for $\chi^{(3)}(\omega, -\omega, \omega)$ in perturbation theory contains

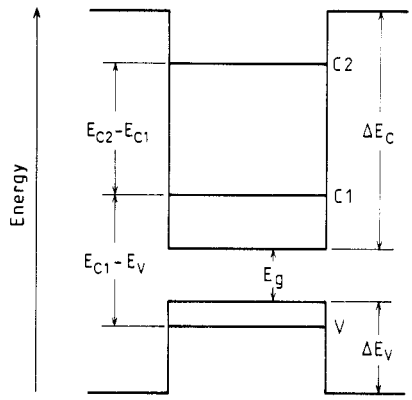

Figure 1. A schematic diagram of the offsets and energies of confined states in a type I semiconductor superlattice. E_g is the band gap of the smaller band gap constituent, ΔE_c is the conduction band offset and ΔE_v the valence band offset. The energy positions of three superlattice states are shown, V is the uppermost valence state and C1 and C2 the first two conduction states. It is seen how, with a large conduction band offset, the energy separation between conduction states, $E_{C2} - E_{C1}$, can be made comparable withthe superlattice fundamental gap, $E_{C1} - E_V$.

terms of the form (Flyzanis 1975, Jha and Bloembergen 1968),

$$\chi^{(3)}(\omega, -\omega, \omega) = \frac{e^4}{V\hbar^3 m^4 \omega^4} \frac{p_{01}p_{12}p_{21}p_{10}}{(\omega_{10} - \omega)(\omega_{20} - 2\omega)(\omega_{10} - \omega)} \tag{1}$$

where $\omega_{ij} = (E_i - E_j)/\hbar$ and p_{ij} is the dipole matrix element between states i and j. This term will become very large if the dipole transitions $0 \rightarrow 1$ and $1 \rightarrow 2$ are allowed and have comparable matrix elements, and $\omega_{10} \approx \omega$, $\omega_{20} \approx 2\omega$. Under such conditions all three denominators in (1) become very small. If we now identify state 0 with V, state 1 with C1 and state 2 with C2 in figure 1, we see that a large enhancement of $\chi^{(3)}(\omega, -\omega, \omega)$ is expected in a direct gap semiconductor structure where the fundamental gap is comparable with the separation between the first two conduction bands, with the energy of the incident radiation tuned just below the band gap, i.e. $E_{C2} - E_{C1} \approx E_{C1} - E_V \approx \hbar\omega$. The conditions required for the enhancement of $\chi^{(3)}$, as considered above, are never fulfilled in natural systems, nor can they be fulfilled in GaAs–$Ga_{1-x}Al_xAs$ quantum well structures.

However, in certain semiconductor superlattices the required combination of allowed transitions and energy separations can be achieved. The criteria for such a situation are shown schematically in figure 1. They involve the combination of a large conduction band offset, small conduction band effective mass and small band gap of one of the constituents. The band line up should be type I in character, i.e. the gap of one constituent lies entirely within the gap of the other. This band line up confines both conduction and valence states in the same material, causing symmetry allowed transitions to have large matrix elements. The conduction band offset needs to be large enough to support at least two confined states. In semiconductor superlattices both transitions V→C1 and C1→C2 are allowed. The transition V→C1 is the across gap transition and is allowed, as it is in bulk materials. The transition C1→C2 is made allowed by momentum mixing caused by the superlattice potential, it is typically of the same order of magnitude as the across gap transition (Brown *et al*

1987). The existence of the transition C1→C2 has also been observed experimentally in GaAs/AlGaAs structures (West and Eglash 1985).

Previously we presented examples of InAs/ZnTe and $Hg_xCd_{1-x}Te$/CdTe superlattices where the spacing of the energy bands meets the above criteria (Morrison *et al* 1989). The nature of the constituents make it difficult to grow well defined interfaces, limiting their practical use. Here we propose a series of superlattices expected to meet the above criteria with optical gaps in the near-infrared region of the spectrum. We consider the $(InAs)_{1-x}(GaSb)_x$/AlSb system. All materials in this superlattice are lattice matched to within $\sim 1\%$ so well defined dislocation-free interfaces should be achievable. The conduction band offset in this system is large (Van de Walle 1989) as required and is represented by the relation $\Delta E_C = 2.01 - 0.88x$ (eV), where x is the alloy concentration. Similarly the valence band offset is represented by the relation $\Delta E_V = 0.56x - 0.1$ (eV). These expressions are obtained by linearly interpolating between the offsets of the InAs/AlSb and GaSb/AlSb interfaces. A type I band alignment is predicted with $x \geq 0.2$.

Table 1. This table contains five different $(InAs)_{1-x}(GaSb)_x$/AlSb superlattices expected to exhibit enhanced third-order optical response due to the mechanism explained in the text. A is the width of the AlSb barrier, each structure has the same barrier width equal to 10 monolayers. B is the width of the $(InAs)_{1-x}(GaSb)_x$ wells and x is the alloy concentration. In each structure the optical gap, $E_{C1} - E_{V1}$, is equal to the separation of the lowest two conduction states, $E_{C2} - E_{C1}$. The optical gaps are seen to span the near-infrared range of the spectrum.

A (Å)	30.4	30.4	30.4	30.4	30.4
B (Å)	30.4	36.5	42.5	48.5	54.7
x	0.88	0.68	0.51	0.36	0.23
Optical gap (eV)	1.103	0.985	0.884	0.800	0.725

In table 1 we present a series of structures predicted to exhibit the criteria $E_{C1} - E_{C2} = E_{C1} - E_{V1}$ in the near-infrared part of the spectrum. The energy separations in these structures are the results of Kronig–Penney effective mass calculations using the above offsets and effective masses of the alloy well material. The effective masses of the lowest bulk conduction band (m_e^*) and heavy hole valence band (m_{hh}^*) of the alloy constituents are, $m_e^*(InAs) = 0.026$, $m_e^*(GaSb) = 0.046$ and $m_{hh}^*(InAs) = m_{hh}^*(GaSb) = 0.40$ (Cardona 1967). Effective masses in the alloy are obtained by interpolating between these values. The parameters in table 1 were obtained by first fixing the well and barrier widths (A and B) and then varying the alloy concentration until the equality in the separation of energy bands is achieved.

3. Transient response

Advances in laser technology over the past decade make it possible to perform spectroscopic experiments on timescales of less than than 100 fs (Flemming and Siegman 1986). Such time resolution is usually achieved by creating ultrashort pulses of laser light and performing pump and probe experiments, i.e. a short pulse of laser light is used to excite the sample and a time delayed pulse used to probe it later (Shah *et al* 1987). For example, time resolved luminescence spectra have been used to estimate the capture times of electrons and holes by semiconductor quantum wells (Deveaud

et al 1988). Also, ultrashort laser pulses have been employed to investigate non-linear optical properties of semiconductors, such as the AC Stark effect observed in semiconductor superlattices (Frohlich *et al* 1987, Knox *et al* 1989, Peyghambarian *et al* 1989). Time resolution in this case makes it possible to distinguish between contributions from real and virtual populations to the AC Stark shift.

Normally, when making theoretical predictions of the optical response of semiconductors, such as those made in section 2, a steady-state response is assumed, i.e. the susceptibilities and absorption coefficients being independent of time . Such steady-state response is established at times much longer than the timescales of typical relaxation processes in the semiconductor. However, at times of order 10–100 fs the semiconductor is exposed to the exciting laser light in the experiments mentioned above the timescale is not long enough to establish a steady-state response. At these ultrashort times Fermi's golden rule of transition rates may no longer hold, i.e. significant absorption may occur at frequencies away from the resonant frequencies of the material (Schiff 1978). This is manifest in a significant broadening of the absorption spectra. It is borne in mind that such effects might be particularly significant in semiconductor superlattices. These structures consist of alternating layers of semiconductors (e.g. GaAs and AlAs) with similar lattice constants and symmetry. The magnitude of the step-like energy difference at the interface determines the degree of confinement of electron and hole levels in one of the constituents (e.g. GaAs). The typical value of this so called conduction and valence band offset is a few tenths of an eV so that the confined levels are separated by a 100 meV or so. The dipole (optical) matrix elements between adjacent levels derived from the conduction band edge of GaAs are large. This creates a novel situation quite unlike anything one can encounter in a bulk material. For example, we find from uncertainty relations that the characteristic time for such transitions is of order $\Delta t = 2\pi h/\Delta E$, where ΔE is the separation between the relevant confined levels. When $\Delta E \sim 10 - 100$ meV, we have $\Delta t \sim 0.4 - 4$ ps. This is to be contrasted with $\Delta t \sim 3$ fs for band gap energy of bulk GaAs.

Here we set out to provide the first basic guidelines for identifying the key spectroscopic features characteristic of superlattices exposed to ultrashort light pulses. We identify the regimes in which the transient nature of the optical response of a semiconductor, and the breakdown of the golden rule become important. We use time-dependent perturbation theory to calculate the first- and second-order absorption effects in semiconductor superlattices at times up to hundreds of fs. We show how in certain superlattices anomalies in the transient response are emphasised. This will set out the limits of applicability of our analysis presented in section 2.

3.1. Method

Our predictions can be understood in terms of a simple three-level model of a semiconductor superlattice consisting of one valence band state, state 0, and the first two conduction bands, states 1 and 2. The energy separations between these states depend on the magnitude of the well/barrier widths and by the type of superlattice constituents. We assume a time-dependent Hamiltonian of the form $H = H_0 + \Delta H$, where H_0 represents the superlattice Hamiltonian and ΔH takes the form

$$\Delta H = (1 - e^{-\alpha t})2H' \sin \omega t \qquad t > 0 \tag{2}$$

$$\Delta H = 0 \qquad t < 0. \tag{3}$$

This represents a harmonic perturbation turned on in a rise time $\tau = 1/\alpha$ from $t = 0$. In the case of radiation, in the dipole approximation, $H' = qAp_x/m_e c$ (the polarisation being in the x direction) where A is the vector potential, p_x the momentum operator in the x direction, q the electronic charge, m_e the electronic mass and c the speed of light (Bassani and Pastori Parravicini 1975). The finite rise time, τ, is necessary as it is unreasonable to think of the perturbation as being instantly turned on. It will be shown later how, if an unreasonably small rise time is assumed, spurious results can be obtained. The value of the rise time chosen in the following calculations is much greater than the period of oscillation but much smaller than the length of the laser pulse.

The time-dependent solution of the full Hamiltonian, Ψ, is described as an expansion in the eigenfunctions of the unperturbed Hamiltonian, H_0,

$$H_0 U_n = E_n U_n \tag{4}$$

$$\Psi = \sum_n a_n(t) U_n \exp(-\mathrm{i}E_n t/\hbar). \tag{5}$$

The coefficients, $a_n(t)$, are expanded as a power series in orders of H'

$$a_n(t) = a_n^{(0)} + a_n^{(1)} + a_n^{(2)} + \ldots. \tag{6}$$

Before $t = 0$ the system is assumed to be in the unperturbed state 0, the uppermost valence state. The method of time-dependent perturbation theory (Schiff 1978) then gives

$$a_n^{(0)}(t) = \delta_{n0} \tag{7}$$

$$a_n^{(1)}(t) = (\mathrm{i}\hbar)^{-1} \langle n|H'|0\rangle F(\omega_{n0}, \omega, t) \qquad n \neq 0 \tag{8}$$

$$a_n^{(2)}(t) = (\mathrm{i}\hbar)^{-2} \sum_{k \neq n,0} \langle n|H'|k\rangle\langle k|H'|0\rangle G(\omega_{nk}, \omega_{n0}, \omega, t) \tag{9}$$

where

$$F(\omega_{n0}, \omega, t) = \frac{1}{\mathrm{i}}\left(\frac{\exp[\mathrm{i}(\omega_{n0}+\omega)t] - 1}{\mathrm{i}(\omega_{n0}+\omega)} - \frac{\exp[\mathrm{i}(\omega_{n0}-\omega)t] - 1}{\mathrm{i}(\omega_{n0}-\omega)}\right.$$
$$\left. - \frac{\exp\{[\mathrm{i}(\omega_{n0}+\omega)-\alpha]t\} - 1}{\mathrm{i}(\omega_{n0}+\omega)-\alpha} + \frac{\exp\{[\mathrm{i}(\omega_{n0}-\omega)-\alpha]t\} - 1}{\mathrm{i}(\omega_{n0}-\omega)-\alpha}\right) \tag{10}$$

and

$$G(\omega_{nk}, \omega_{n0}, \omega, t) = \int_0^t \exp(\mathrm{i}\omega_{nk}t')[1 - \exp(-\alpha t')]2\sin\omega t'\, F(\omega_{n0}, \omega, t')\, \mathrm{d}t' \tag{11}$$

(ω_{nk} is defined as $(E_n - E_k)/\hbar$). Integration of the time-dependent factor in the second-order coefficient, G, is very tedious and involves 32 terms in total, hence numerical integration was employed when evaluating it.

3.2. First-order effects

In order to demonstrate the transient nature of the response to first order in the field at ultrashort times, we consider a system in which $\omega_{21} \ll \omega_{10}$ and excite it with radiation at the resonant frequency $\omega = \omega_{10}$. This represents a superlattice in which the lowermost conduction bands, represented by states 1 and 2, are closely spaced in energy. We then calculate the expectation value of the electronic dipole to first order in the applied field,

$$\langle qx \rangle^{(1)} = \langle \Psi^{(0)} | qx | \Psi^{(1)} \rangle + \text{CC} \tag{12}$$

where $\Psi^{(0)}$ and $\Psi^{(1)}$ represent the zeroth- and first-order wavefunctions respectively and q is the electronic charge. With the definitions of $a_n^{(0)}$ and $a_n^{(1)}$ in (7) and (8), and with $H' = qAp_x/m_e c$, this can be written as

$$\langle qx \rangle^{(1)} = \sum_n |\langle n|p_x|0\rangle|^2 \frac{Aq^2}{\hbar c m_e^2 \omega_{n0}} \exp(-\mathrm{i}\omega_{n0}t) F(\omega_{n0}, \omega, t) + \text{CC}. \tag{13}$$

Here CC represents the complex conjugate of the first part of the equation and use has been made of the commutation relation (Merzbacher 1970)

$$\langle m|x|n\rangle = \frac{\mathrm{i}\langle m|p_x|n\rangle}{\omega_{nm} m_e} \qquad m \neq n. \tag{14}$$

We now consider contributions to the expectation value of the first-order dipole from the two excited states of the three-level system and write

$$\langle qx \rangle^{(1)} = D_1 + D_2 \tag{15}$$

D_1 and D_2 being the contributions due to states 1 and 2 respectively.

First of all, consider the contribution from state 1, D_1. At times much greater than the rise time, $t \gg 1/\alpha$ (assumed much greater than the period of the radiation), we can approximate

$$F(\omega_{10}, \omega = \omega_{10}, t) \simeq \mathrm{i}t. \tag{16}$$

This contributes the term

$$D_1 \simeq \frac{Aq^2 t}{\hbar c m_e^2 \omega} |\langle 1|p_x|0\rangle|^2 2 \sin \omega t \tag{17}$$

to the total first-order dipole, i.e. a sinusoidal term with the same frequency as the perturbing field. At long times this term will dominate, contributions from other states away from resonance becoming increasingly insignificant as time increases. This is the long time limit where the golden rule applies.

However, at very short times there is a significant term due to state 2, D_2. Assuming $\omega_{21} \ll \omega_{10}$ we can write

$$F(\omega_{20}, \omega, t) \simeq \frac{\mathrm{i}[\exp(\mathrm{i}\omega_{21}t) - 1]}{\omega_{21}}. \tag{18}$$

This is a slowly varying function in time, as ω_{21} is assumed small. The electronic dipole contribution from state 2 can now be written

$$D_2 \simeq \frac{iAq^2|\langle 2|p_x|0\rangle|^2 i}{\hbar c m_e^2(\omega+\omega_{21})}\exp(-i\omega t)\frac{1-\exp(-i\omega_{21}t)}{\omega_{21}} + \text{CC.} \tag{19}$$

This represents a sinusoidal function with the frequency of the applied field, ω, modulated by a slowly varying function with frequency ω_{21}. This term will be significant when the ratio $|D_2/D_1|$ is large. We can approximate,

$$|D_2/D_1| \simeq 1.0/\omega_{21}t \tag{20}$$

where both momentum matrix elements, $\langle 2|p_x|0\rangle$ and $\langle 1|p_x|0\rangle$, have been assumed to be allowed and approximately equal. For time in the range of 100 fs this gives a $|D_1/D_2|$ close to unity if $\hbar\omega_{21}$ is in the range of 10 meV.

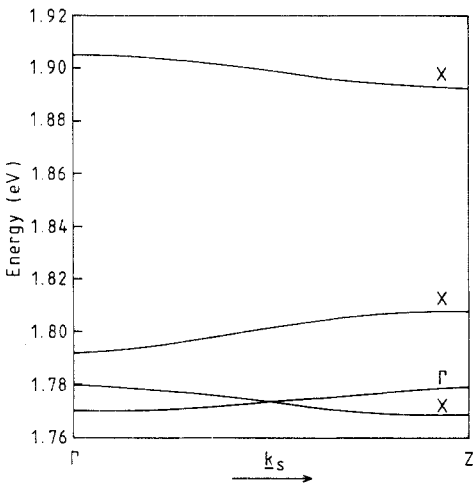

Figure 2. The dispersion along the Γ–Z of the first three conduction bands of the GaAs–AlAs structure described in the text. Γ–Z is the line in the superlattice Brillouin zone from the centre to the edge in the direction of growth (001). The bands are labelled Γ and X describing which minima of the bulk band structure they originate from. Note the closeness in energy of the first two bands at the centre of the superlattice Brillouin zone (Brown *et al* 1987).

As a specific example of a structure where this effect will be prominent consider the GaAs–AlAs superlattice whose period consists of 12 monolayers of GaAs and 8 monolayers of AlAs. The band structure of this superlattice has been obtained from a full scale pseudopotential calculation with the inclusion of spin–orbit coupling (Brown *et al* 1987). The lowest conduction bands of the superlattice are plotted, along the Γ–Z line in the superlattice Brillouin zone, in figure 2. At the centre of the superlattice Brillouin zone the separation of the first two conduction bands is seen to be approximately 10 meV and the band gap 1.77 eV. As described above, in order that the contribution to the expectation value of the first-order dipole, $\langle ex\rangle^{(1)}$, from state 2 (the second superlattice conduction band) be important, the momentum matrix elements between the uppermost superlattice valence state, state 0, and the lowermost

superlattice conduction states, states 1 and 2, at the centre of the superlattice zone, need to be comparable. If these matrix elements, $\langle 2|p_x|0\rangle$ and $\langle 1|p_x|0\rangle$, are both large and the superlattice is illuminated by radiation at the resonant frequency ω_{10}, at ultrashort times the contribution to the expectation value of the first-order dipole due to the presence of state 2 will be important.

The existence of two superlattice states close in energy and both having allowed momentum matrix elements to states at the valence band maxima is unusual but is achieved here due to momentum mixing in the superlattice conduction states. To explain this a brief description of the method of calculation employed to obtain the band structure in figure 2 is needed. In the calculation, the superlattice wavefunctions, Ψ_S, are written as a linear combination of bulk Bloch states of GaAs, $\varphi(n,k)$:

$$\Psi_S = \sum_{nk} A(n,k)\varphi(n,k). \tag{21}$$

Here n represents the bulk band index and k the reduced wavevector in the bulk Brillouin zone. The values of k in the expansion are uniquely determined by the periodic boundary condition given by the superlattice period. The uppermost superlattice valence states are constructed from the bulk zone-centre ($k = 0$) Bloch states of the uppermost GaAs valence band. Superlattice states with large momentum matrix elements to this state require significant contributions to their wavefunctions from the bulk zone-centre Bloch states of the lowermost GaAs conduction band (Brown *et al* 1987). This is due to the strong allowed vertical transition across the gap in bulk GaAs.

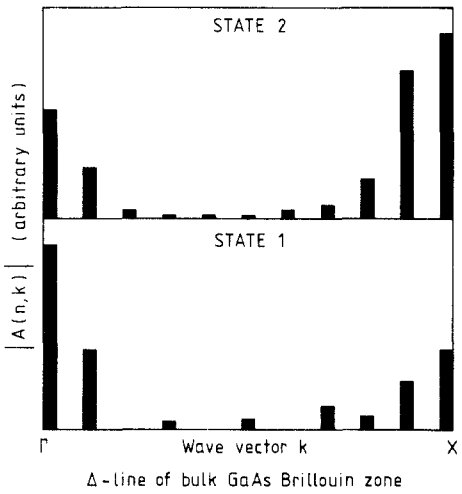

Figure 3. Plots of the expansion coefficients associated with the lowest two conduction states at the centre of the superlattice Brillouin zone, see figure 2. Only contributions from the lowest conduction band of GaAs are shown, contributions from other bands being insignificant for the states in question. Note how both states are derived from a mixture of GaAs Bloch states from the bulk Γ and X minima. The states are said to be significantly mixed in momentum space. The large contributions from the GaAs bulk Γ minimum result in allowed optical transitions to the uppermost valence state in both cases.

In figure 3 we plot the expansion coefficients associated with the first two superlattice states at the superlattice zone centre. Both states are seen to have significant

contributions from the lowest GaAs conduction band zone-centre states, along with significant contributions from the GaAs zone-edge states—the states are said to be mixed in momentum space. This means both states have large momentum matrix elements to the uppermost superlattice valence state.

The expectation value of the first-order dipole, with the incident radiation at the resonant frequency $\omega = \omega_{10} = 1.77$ eV, as a function of time, is plotted in figure 4. The rise time is 20 fs and momentum matrix elements from the uppermost valence band to the first two superlattice conduction band states at the superlattice zone centre are assumed equal. At very short times the slowly oscillating contribution due to the proximity of state 2 is clearly seen to be important. At longer times the contribution from state 2 becomes dwarfed by the contributions from state 1.

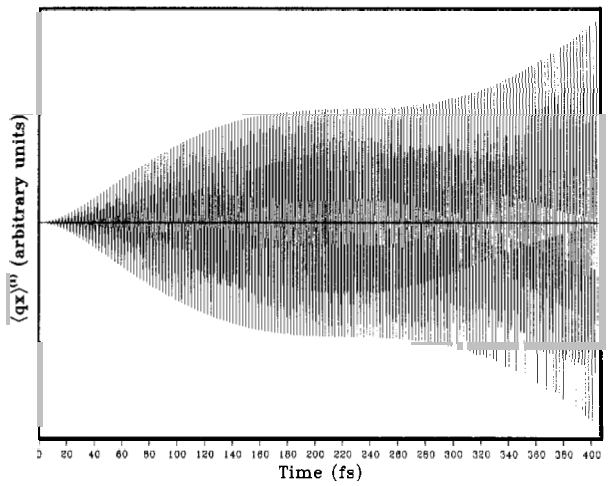

Figure 4. The calculated expectation value of the first-order dipole in a system with $\hbar\omega_{10} = 1.77$ eV and $\hbar\omega_{21} = 10$ meV as a function of time. The radiation field is tuned to the resonance ω_{10}. The slowly oscillating component of the response due to state 2, the second conduction band state, is clearly seen to be important at ultrashort times.

3.3. Second-order effects

To show the relative importance of second-order effects at ultrashort times we consider the second-order transition probabilities, $|a_k^{(2)}|^2$, and compare them to first-order transition probabilities, $|a_k^{(1)}|^2$. As previously stated, the second-order coefficients are calculated by the numerical integration of (11). The importance of including the factor $(1 - e^{-\alpha t})$ in the harmonic perturbation becomes apparent when calculating the second-order coefficients. If the rise time, $\tau = 1/\alpha$, is made very short (shorter than the period of the radiation) spurious maxima appear in the second order coefficient at frequency $\omega = \omega_{21}$.

This is shown in figures 5(a) and (b) where the magnitude of the second-order coefficient $|a_2^{(2)}|$ is plotted as a function of the frequency of the incident radiation, ω. The system is modelled with $\hbar\omega_{10} = 600$ meV, $\hbar\omega_{21} = 400$ meV and time $t = 100$ fs. Two values of the rise time, τ, are considered (a) $\tau = 1$ fs and (b) $\tau = 20$ fs. In both cases we see the principle maxima at $\hbar\omega = \hbar\omega_{20}/2 = 500$ meV, corresponding

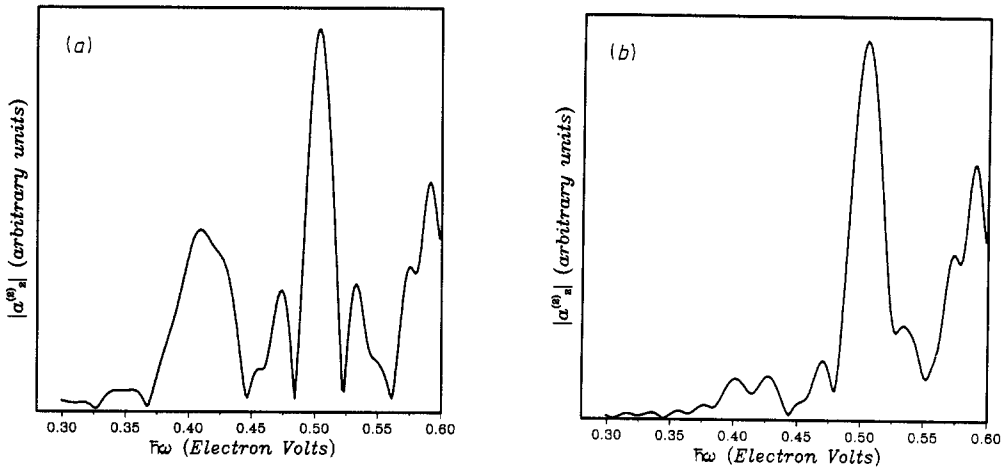

Figure 5. Two plots of $|a_2^{(2)}|$, for example, in a system with $\hbar\omega_{10} = 600$ meV and $\hbar\omega_{21} = 400$ meV as a function of the energy of the incident radiation, $\hbar\omega$. The time of calculation for both plots is 100 fs. In (a) the rise time, τ, is 1 fs and in (b) τ is equal to 20 fs. It is clearly seen how the secondary maximum at $\hbar\omega = \hbar\omega_{21}$ is drastically reduced as the rise time is increased.

to two-photon absorption. In case (a) there is also a secondary maxima at $\hbar\omega = \hbar\omega_{21} = 400$ meV, this maxima is seen to be much reduced in case (b) where the rise time is much longer. In order to eliminate effects due to this secondary maxima a rise time of 20 fs is chosen in the following calculation. We should also note the finite widths of the principle maxima at finite times. Second-order two-photon absorption is important at frequencies significantly away from the resonant frequency $\omega = \omega_{20}/2$ at the ultrashort times considered here.

To emphasise the width of the second-order absorption peak and the relative importance of first-order and second-order processes at ultrashort times, we consider a three-level system with $\hbar\omega = \hbar\omega_{20}/2 = 0.5$ eV and calculate $|a_2^{(2)}|^2$ as a function of $\hbar\omega_{10}$. The results of this calculation at time $t = 100$ fs are plotted in figure 6. The maximum of $|a_2^{(2)}|^2$ is seen to be at $\omega_{10} = \omega$, as expected. The magnitude of $a_2^{(2)}$ is large when ω_{10} is close to ω as state 1 then acts as a virtual state close to resonance in the two-stage process of excitation to state 2. The half width of the peak in figure 6 is $\sim h/t$, this relation will continue to times comparable with typical relaxation times in semiconductors, after which the width will be dominated by relaxation processes. Typical relaxation times are much greater than the 100 fs timescale considered in this study. In the limit of very large times the peak in figure 6 will become very narrow, second-order absorption becoming insignificant except at $\omega_{10} = \omega$. However at finite times the peak is seen to be significantly broadened. In the case considered in figure 6 ($t = 100$ fs) the width of the peak is approximately 100 meV, i.e. significant second-order absorption results when $\hbar\omega_{10}$ is in the energy range $\hbar\omega_{20}/2 \pm 50$ meV.

We have seen previously that a superlattice in which the second-order absorption is significant at ultrashort times requires that the band gap energy, $\hbar\omega_{10}$, is equal to the separation of the first two conduction states, $\hbar\omega_{21}$, within the energy width of the peak of the principal maximum in $|a_2^{(2)}|^2$, see figure 6. For times of 100 fs this width is approximately 100 meV. Such criteria of the band separation in a superlattice

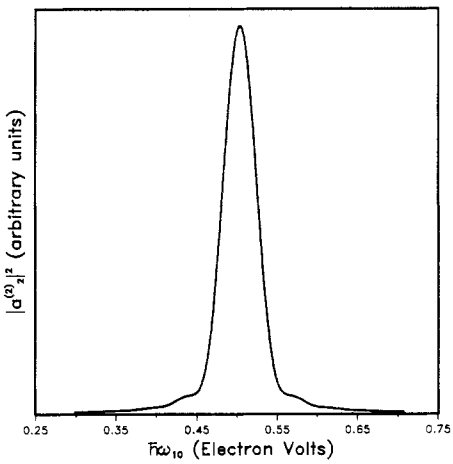

Figure 6. The calculated value of $|a_2^{(2)}|^2$, for example, in a system with an incident radiation frequency $\hbar\omega = \hbar\omega_{20}/2 = 0.5$ eV as a function of the energy separation $\hbar\omega_{10}$. The time is 100 fs and the rise time 20 fs. The finite width of the peak at this ultrashort time is clearly seen. At longer times the width of the peak will narrow approaching the delta function limit.

can be achieved in a system with has a large conduction band offset and small band gap of one of the constituents, see figure 1. The band gap line up should be type I in character, i.e. the gap of one constituent lies entirely within the gap of the other. This band line up confines both conduction and valence states in the same material, causing symmetry allowed transitions to have large matrix elements. The conduction band offset needs to be large enough to support at least two confined states. The large offset causes the separation between the confined states to be reasonably large. These are the same criteria for the enhancement of $\chi^{(3)}$ as described in section 2.

To emphasise further the importance of second-order absorption we consider the resonant case where $\omega_{10} = \omega = \omega_{21}$ and calculate the ratio of the probability of a second-order transition to state 2, $|a_2^{(2)}|^2$, to the probability of a first-order transition to state 1, $|a_1^{(1)}|^2$. At the resonant conditions, $\omega = \omega_{10} = \omega_{21}$ we can approximate the functions F and G, see (10) and (11), by

$$F(\omega_{10}, \omega, t) \simeq it \tag{22}$$

and

$$G(\omega_{21}, \omega_{10}, \omega, t) \simeq t^2/2. \tag{23}$$

Thus we can write,

$$\frac{|a_2^{(2)}|^2}{|a_1^{(1)}|^2} \simeq |\langle 2|p_x|1\rangle|^2 \left(\frac{qE_0 t}{2\hbar m\omega}\right)^2 \tag{24}$$

where we have used the relation $A_0 = cE_0/\omega$, E_0 being the electric field strength.

We assume that the matrix element $\langle 2|p_x|1\rangle$ represents an allowed transition. We have shown that in such cases the magnitude of a typical matrix element is 0.1 atomic

units. Equation (24) now shows that, at times of the order of 100 fs, and using a resonant frequency typical for the structures proposed in section 2 ($\sim$ 0.5 eV), the second-order absorption will be comparable with first-order absorption at field strengths of the order 5×10^5 V cm^{-1}. Such field strengths correspond to a laser intensity of 0.3 GW cm^{-2}, well within the range of the current technology.

3.4. Transient effects in superlattices with large non-linearity

The results of subsections 3.1–3.3 show that the breakdown of Fermi's golden rule at ultrashort times causes deviations from the non-linear optical behaviour predicted by steady-state theory. With radiation tuned slightly below the band gap energy, the degree of anomalous response depends on the energy separation of the superlattice conduction subbands. We have shown how, at times of 100 fs, large deviations are expected from the results predicted by the golden rule when the conduction band energy separations are of the order of tens of meV. The effect due to the breakdown of the golden rule at ultrashort times in semiconductor superlattices has not been previously considered in the literature. For example, Khurgin (1988) has presented the results of calculations on the non-linear optical properties of asymmetric $Ga_{1-x}Al_xAs$–GaAs quantum well structures where the steady-state formalism is adopted. In the structures he considered the separation of conduction states is of the order 10–100 meV. Deviations from the results predicted by Khurgin are expected if experiments are performed with timescales of 100 fs. It is important to realise that the physical mechanism (i.e. the virtual transitions) responsible for non-linear response in SEED (Miller 1989), or asymmetric well structures, is quite unlike that proposed in section 2. In the structures presented in section 2, where the predicted enhanced non-linear optical properties is caused by virtual excitations to the higher conduction bands, the separation of the lowest conduction bands in the InAs–ZnTe and $Hg_xCd_{1-x}Te$ structures are 0.64 eV and 0.39 eV respectively. These conduction band energy separations are large enough so that deviations from the golden rule will be unimportant at times of 100 fs and the conventional (steady-state) formalism will suffice to predict their non-linear optical properties. The broadening of the maxima of the second-order coefficients at ultrashort times predicted in subsection 3.3 is also useful for characterisation of materials expected to possess large virtual third-order susceptibility. The transitions involved in the second absorption are the same as the virtual transitions considered in section 2 which contribute to the third-order susceptibility. The broadening of the maxima, see figure 6, means that even if a certain difference in the energy separations exist between $E_{C2} - E_{C1}$ and $E_{C1} - E_V$ the material may still exhibit an enhanced third-order susceptibility. This energy difference at 100 fs is $\sim$ 50 meV. Such a broadening of course competes with the contributions due to the relaxation and dispersion processes which are usually considered in the literature (Wherret 1983).

Finally, it is worth pointing out that the three-level model we have chosen as a basis of our estimate of the main steady state as well as transient non-linear properties *is* realistic in the structures in question. This is *unlike* the physical situation which arises in the case of, say, optical Stark phenomena in GaAs quantum wells (Chemla 1988, Frohlich *et al* 1987, Knox *et al* 1989, Peyghambarian *et al* 1989). There the gap energy greatly exceeds the energy separation of the lowest confined levels and a large number of higher-lying resonances may affect both the Stark shifts and transients. Quite the opposite happens in the structures proposed in section 2. The near gap radiation preferentially engages only the adjacent subbands whose dipole matrix element with each other is large, the other levels either do not have the correct energy, parity or

momentum (Brown *et al* 1987) to compete efficiently with the contributions of the dominant three levels.

4. Conclusions

We have shown how virtual transitions to higher superlattice subbands can lead to a significant enhancement of the third-order non-linear susceptibility. The basic requirement for a large enhancement to $\chi^{(3)}$ is that the fundamental band gap energy be comparable with the separation between the lowest superlattice conduction subbands. Under such conditions a large enhancement of $\chi^{(3)}$ is expected with the exciting radiation detuned slightly below the band gap energy. The criteria needed to achieve such a superlattice band structure have been laid down and specific examples of $(InAs)_{1-x}(GaSb)_x/AlSb$ superlattices, where the effect should be observable in the near-infrared region of the spectrum, have been presented.

We have also presented a study of the non-linear optical properties of such superlattices subjected to ultrashort pulses of laser light. We show that at times of the order 100 fs modifications are needed to the steady-state formalism of non-linear response only if the separation of conduction bands is of the order 10-100 meV. The steady-state formalism is adequate at times of order 100 fs in structures with conduction subband separation greater than 100 meV, this includes the structures presented in section 2. Naturally, the model used here to make predictions concerning the transient nature of the optical response in semiconductors is greatly oversimplified. For example, we have ignored the detailed character of relaxation processes. Other effects such as details of band dispersion and the width of the applied laser beam may also affect the quantitative aspects of the predictions of this paper. However, we believe that the main features of the transient optical response in the systems considered here is described realistically enough to ensure that our predictions are qualitatively correct.

Acknowledgments

We would like to thank the Science and Engineering Research Council (UK), Procurement Executive MOD/RSRE Malvern, and ONR (contract no N00014-88-J-1003) for financial support.

References

Bassani F and Pastori Parravicini G 1975 *Electronic States and Optical Transitions in Solids* (Oxford: Pergamon) p 152

Brown L D L, Jaros M and Ninno D 1987 *Phys. Rev.* B **36** 2935

Cardona M 1967 *Semiconductors and Semimetals* vol 3 *Optical Properties of III–V Compounds* ed R K Willardson and A C Beer (New York: Academic) p 151

Chang Y C 1985 *J. Appl. Phys.* **58** 499

Chemla D S 1988 Excitonic optical non-linearities in semiconductor quantum wells *Laser Optics of Condensed Matter* ed J L Birman *et al* (New York: Plenum) p 71

Deveaud B, Shah J, Damen T C and Tsang W S 1988 *Appl. Phys. Lett.* **52** 1886

Flemming G P and Siegman A E (ed) 1986 *Ultrafast Phenomena* vol 5 (Berlin: Springer) p 1

Flyzanis C 1975 *Quantum Electronics* vol 1A (New York: Academic) p 87

Fong C Y and Shen Y R 1975 *Phys. Rev.* B **12** 2325

Frohlich D, Wille R, Schlapp W and Weimann G 1987 *Phys. Rev. Lett.* **59** 1748
Haug H 1988 *Optical Nonlinearities and Instabilities in Semiconductors* (New York: Academic) p 5
Haug H and Schmitt-Rink S 1985 *J. Opt. Soc. Am.* B **27** 1135
Jha S S and Bloembergen N 1968 *IEEE J. Quantum Electron.* **QE-4** 670
Kelly P L 1963 *J. Phys. Chem. Solids* **24** 607
Khurgin J 1988 *Phys. Rev.* B **38** 4056
Knox W H, Chemla D S, Miller D A B, Stark J B and Schmitt-Rink S 1989 *Phys. Rev. Lett.* **62** 1189
Merzbacher E 1970 *Quantum Mechanics* (New York: Wiley) p 338
Miller D A B 1989 *Appl. Phys. Lett.* **54** 202
Morrison I, Jaros M and Beavis A W 1989 *Appl. Phys. Lett.* **55** 1609
Peyghambarian N, Koch S W, Lindberg M, Fluegel B and Joffre M 1989 *Phys. Rev. Lett.* **62** 1185
Schiff L I 1978 *Quantum Mechanics* (New York: McGraw-Hill) p 280
Shah J, Damen T C, Deveaud B and Block D 1987 *Appl. Phys. Lett.* **50** 307
Shen Y R 1984 *The Principles of Nonlinear Optics* (New York: Wiley) p 1
Thylén L 1988 *J. Lightwave Technol.* **6** 847
Van de Walle C G 1989 *Phys. Rev.* B **39** 1871
West L C and Eglash S J 1985 *Appl. Phys. Lett.* **46** 1156
Wherret B S 1983 *Proc. R. Soc.* A **390** 373
Wolff P A, Yuen S Y, Harris K A, Cook J W Jr and Schetzina J F 1987 *Appl. Phys. Lett.* **50** 1858